Study on a novel hydroxamic acid as the collector of rhodochrosite

Gang Zhao [1, 2], Ting Dai [1, 2], Shuai Wang [1, 2], Hong Zhong [1,2]

[1] College of Chemistry and Chemical Engineering, Central South University, Changsha, 410083, China

[2] Hunan Provincial Key Laboratory of Efficient and Clean Utilization of Manganese Resources, Central South University, Changsha, 410083, China

Corresponding authors: wangshuai@csu.edu.cn (Shuai Wang), zhongh@csu.edu.cn (Hong Zhong)

Abstract: A novel collector, tert-butyl benzohydroxamic acid (TBHA), was first introduced in rhodochrosite flotation. The performance of TBHA was investigated by the density functional theory (DFT) calculation along with the micro flotation test, zeta potential determination and XPS analysis, compared with benzohydroxamic acid (BHA). TBHA has stronger affinity to the mineral than BHA in terms of frontier molecular orbital, atomic net charge and bond population. The substitution of tert-butyl group on the benzene ring improves the affinity of the hydroxamic acid to the mineral. TBHA exhibits excellent collecting ability to rhodochrosite with a recovery of about 99% at a concentration of 3.89×10^{-4} mol/dm³ and pH 6.5. The hydroxamic acid molecules are adhered on mineral surfaces by chemical adsorption, resulting in negative shifts for the zeta potential of rhodochrosite with the presence of the collector. Chemical adsorption can be also confirmed from XPS analyses that the atomic concentration ratios of C and O to Mn on the treated mineral surfaces were increased and the binding energy of Mn3s was decreased. The experimental data achieve excellent agreement with the computational analyses.

Keywords: flotation, rhodochrosite, hydroxamic acid, DFT

1. Introduction

Rhodochrosite (MnCO₃), an important manganese ore, is one of the resources for electrolytic manganese production. More than 90% of the resources are classified as low-grade manganese ores with complicated composition and finely disseminated grain in China. So the beneficiation for rhodochrosite ores is very necessary before further mineral processing. Froth flotation, regarded as an effective and favorable mineral beneficiation method, shows various advantages over the other techniques in terms of applicability, operability, efficiency and economy (Nagaraj and Farinato, 2016; Sousa et al., 2017). In froth flotation, collectors play a critical role upon the improvement of mineral floatability. Traditional collectors, including oleic acid, oxidized paraffin wax soap and other anionic organic compounds, have been used for rhodochrosite flotation but the results from these collectors are far from satisfactory (Fuerstenau and Shibata, 1999). So these problems are desiderated to be solved by the development of novel collectors with high efficiency.

As widely considered, computational methods such as density functional theory (DFT) are valuable tools for understanding the chemical reactivity systems to elucidate the possible interaction mechanisms hidden in experimental findings (Parr and Yang, 1984; Ayers and Parr, 2000; Yang et al., 2003). As a result, the theoretical calculation based on DFT method was adopted to study the structure-activity relationship of the collectors. Hydroxamic acids are a kind of effective organic ligands containing -C(=O)NHOH group, in which both O and N atoms are recommended as coordination atoms in all kinds of complexes. The characteristic structure of hydroxamic acids determines its strong chelating ability to metal ions, such as Cu, Ni, Co, Fe and Zn, etc (Farkas et al., 2007; Griffith et al., 2011; Ali and Fridgen, 2011). In the light of these advantages, hydroxamic acids have attracted more and more attention used as chelating collector in various kinds of oxidized ores

such as scheelite (Han et al., 2017), cassiterite (Wu and Zhu, 2006), rare earth (Jordens et al., 2016), etc. However investigations on the interaction of hydroxamic acid with rhodochrosite were not systematically clarified and very limited information was available in the references. In the development of novel hydroxamic acids, Zhou et al. have done some meaningful work that they designed a novel linoleate hydroxamic acid (LHA) and tested its performance on rhodochrosite flotation (Zhou et al., 2015a and 2015b). The novel collector achieved superior flotation indices compared with oleic acid that 97% rhodochrosite could be collected by LHA. The FT-IR spectra show that the collector-mineral complexes with five-membered chelate ring were formed on mineral surfaces. Aromatic hydroxamic acids are also an important category of commonly used collectors in the flotation practice, such as benzohydroxamic acid (BHA), which is the most widely applied phenyl hydroxamic acid.

In our previous work, we have studied a naphthenic hydroxamic acid (cyclohexyl hydroxamic acid, CHA) as the collector in the flotation of tungsten ore. The performance of CHA was approved to be better in the flotation of scheelite compared with benzohydroxamic acid (BHA) that the collecting ability of CHA to scheelite is stronger from both experimental and computational results (Zhao et al, 2013). In this work, a novel aromatic collector, tert-butyl benzohydroxamic acid (TBHA), was introduced as the collector for rhodochrosite flotation. The alkyl group is generally recognized to be electron-donating group. The substitution of tert-butyl on phenyl group is supposed not only to increase the hydrophobicity of the collector but also improve the electron donating ability of the functional group. On the other hand, the novel hydroxamic acid can be easily synthesized from 4-tert-butyl benzoic acid (one of the important chemical intermediates) through esterification and oximation reactions. The collecting performance of TBHA would be investigated by DFT calculations, micro flotation, zeta potential and X-ray photoelectron spectroscopy (XPS). Additionally, the flotation efficiency of TBHA and BHA would be analyzed contrastively from the structure characteristics and electronic properties.

2. Material and methods

2.1 Computational

All the calculations were performed on Gaussian 09 package (Frisch et al., 2009). Molecular structures were optimized with DFT method at B3LYP/6-311+G** level (Gece and Bilgiç, 2010; Liu et al., 2012). Energies were calculated with the same basis set. To optimize the molecular structure in aqueous solution, IEF-PCM (the integral equation formalism for the polarizable continuum) model was adopted. The atom net charge and bond order were obtained from natural population analysis. For free Mn^{2+} ion ($3d^5$), the d-electrons are well-distributed in the five d-orbitals. So the spin multiplicity of the free Mn^{2+} ion is 6 in the calculation settings. For Mn^{2+} ion in the complexes, the d-orbitals split owing to the influence by ligands (collectors). Based on the crystal field theory, the Crystal Field Stabilization Energies (CFSE) of square configuration complexes formed by metal ions with d^5 electron configuration in low spin state is the largest compared with tetrahedron and octahedron configurations, that is, the square configuration is most stable. In low spin state, there is one single electron for Mn^{2+} in the complexes, so the spin multiplicity of the complexes is 2 in the calculation settings

2.2 Materials

The single mineral was characterized by chemical analysis and X-ray diffraction (XRD) to analyze the compositions. The concentration of Mn in mineral sample is 42.7% and the mineral purity is 89.3%. The ores were ground to 0.037 ~ 0.076 mm, washed by distilled water and then dried for flotation tests. The X-ray diffraction pattern of the mineral sample is shown in Fig. 1.

2.3 Micro flotation

Flotation tests were carried out in a laboratory flotation cell (XFG, Jilin Prospecting Machinery Factory, China) with a volume of 40 cm³ (Gao et al, 2016a, b). In each test one sample (2.0 g single mineral) was dispersed with distilled water. The pH was adjusted by diluent hydrochloric acid or sodium hydroxide. Then the collector was introduced and the pulp was conditioned for 3 min,

followed by scraping for 5 min. The floated and unfloated particles were collected, respectively. The flotation recovery was calculated based on solid weight distributions between the two products. Each test under the same condition was carried out for three times and the average data were reported.
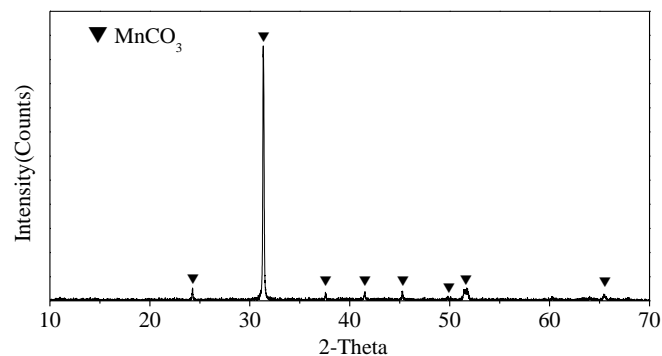

Fig. 1. XRD of rhodochrosite sample used in this study

2.4 Zeta potential measurement

The zeta potential was measured by analyzing finely ground mineral powders (-5 µm) in distilled water using Zeta Potential Analyzer (ZetaPALS, Brookhaven Instruments Corporation, USA). The pH was adjusted with dilute nitric acid or sodium hydroxide. The concentration of TBHA is 3.11×10^{-4} mol/dm^3. The zeta potential was obtained from the Smoluchowski equation. The reported zeta potential was averaged from five runs including ten cycles.

2.5 X-ray photoelectron spectroscopy

X-ray photoelectron spectroscopy (XPS) were recorded on a Thermo Scientific ESCALAB 250Xi using Al Kα X-ray source operated at 200 W with 20 eV pass energy. The vacuum pressure is ranged from 10^{-9} to 10^{-8} Torr and the takeoff angle is 90°. The data were collected and processed under Thermo Scientific Avantage 5.52 software. The carbon contamination peak at 284.0 eV was used to account for charging a sample. For rhodochrosite treated by TBHA, the sample was cleaned using distilled water several times to wash off the residual collector.

3. Results and discussion

3.1 DFT study on collector reactivity

The mainly reported two tautomers for hydroxamic acids, amide form and oxime form, are shown in Fig. 2, on which the atom numbers are labeled, where R represents the alkyl group. There are also *E-Z* configurations for hydroxamic acid molecules in stereochemistry. The possible conformers for BHA and TBHA molecules are shown in Table 1 and the Gibbs energies of each conformer are listed below. The order of stabilities is *Z*-amide > *E*-amide > *Z*-oxime > *E*-oxime for both BHA and TBHA molecules. The *Z*-amide form is found to be the most stable one in the aqueous phase, in agreement with the results reported by Arora et al. (2017).

3.2 Molecular geometry

The optimized molecular geometries of the *Z*-amide conformer for BHA and TBHA are shown in Fig. 3, labeled with the element symbols for C, N, and O taking BHA molecule for example.

As shown in Fig. 3, the conjugate -C(=O)-NH-OH group improves the electron delocalization itself, which may result in a stronger ability to accept the back donation electron from mineral metals, such as manganese. The dihedral angles of O-C-N-O atoms in the molecules (anions) are 7.816° (1.632°) and 7.970° (1.619°) for BHA and TBHA, respectively. The dihedral angles of O-C-N-O for anions are much smaller that the four atoms are almost in a plane for both BHA and TBHA. Such a planar configuration favors the formation of conjugated π or π* bond which is convenient to donate electrons to the empty d-orbitals of metal atoms in mineral surfaces.
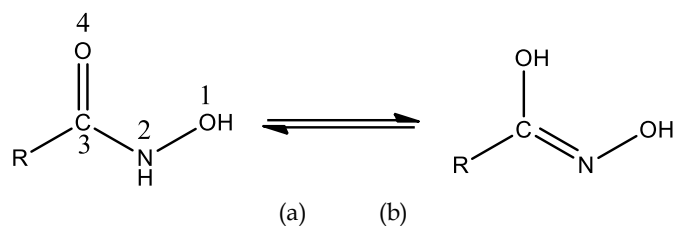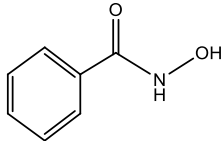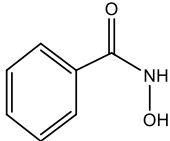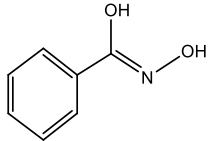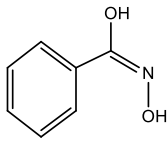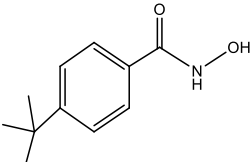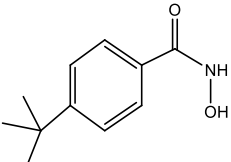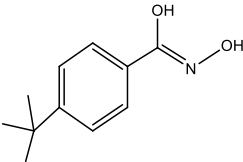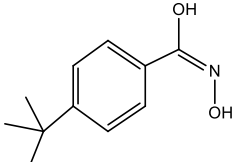
Fig. 2. Two tautomers of hydroxamic acids: (a) amide and (b) oxime

Table 1. Various conformers for BHA and TBHA and the Gibbs energies (a.u.)

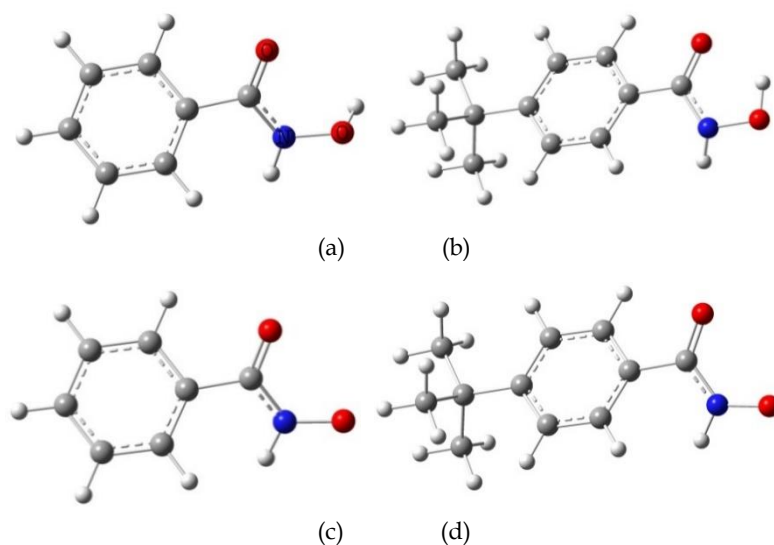| Species	Z-amide	E-amide	Z-oxime	E-oxime
BHA	-476.261851	-476.259033	-476.257484	-476.247688
TBHA	-633.561876	-633.555733	-633.554108	-633.544634

Fig. 3. The optimized geometries of BHA molecule (a), TBHA molecule (b), BHA anion (c) and TBHA anion (d)

3.3 Charge population

Molecular electrostatic potential (MEP) simultaneously and visually displays a molecular size and shape as well as positive, negative and neutral electrostatic potential regions in terms of color grading. It describes the electron density in the target molecule. In the majority of the MEP maps, red and blue represent the regions with the most negative and most positive electrostatic potentials, respectively. The color coding of these maps is in the range between -0.05 a.u. (deepest red) and 0.05 a.u. (deepest blue), as shown in Fig. 4. The negative charge covers the oxygen atoms, and the positive region is mainly over the hydrogen atom adjacent to the nitrogen atom for both BHA and TBHA. The value of the electrostatic potential is largely responsible for the binding sites of a substrate to its receptor because the receptor and corresponding ligand recognize each other at their molecular surfaces.

Consequently, the higher electronegativity in the two oxygen atoms makes them the most reactive parts in the molecule for denoting electrons to the receptor (such as minerals) forming five-membered chelate rings (Liu et al., 2006).
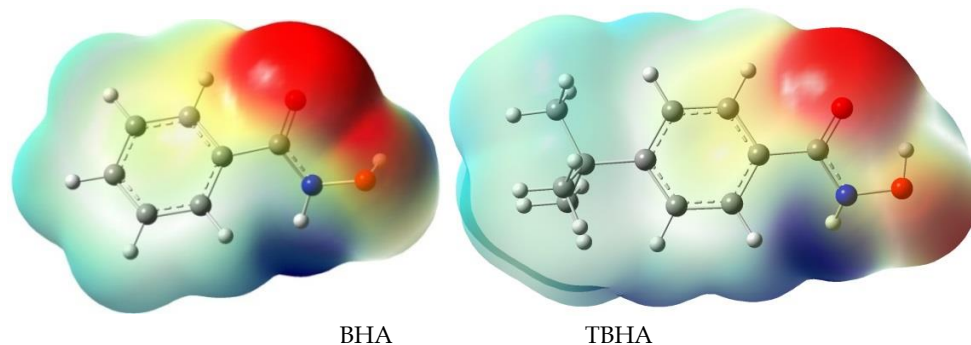

BHA   TBHA

Fig. 4. MEP plots of BHA and TBHA molecules

The atomic net charge in hydroxamic group obtained from natural charge population is listed in Table 2. More negative charge in the oxygen atoms enables TBHA stronger affinity to metal atoms on mineral surfaces, compared with BHA.

Table 2. Natural charge assigned to the heavy atoms in hydroxamic groups

Species	Natural charge of the atoms in hydroxamic groups				
	O1	N2	C3	O4	O1+O4
BHA	-0.554	-0.310	0.640	-0.682	-1.236
TBHA	-0.563	-0.312	0.635	-0.689	-1.252

3.4 Frontier molecular orbitals

Frontier molecular orbital (FMO) theory supposes that the occupied orbitals of one molecule and the unoccupied orbitals of the other interact with each other causing attraction, especially for the highest occupied molecular orbital (HOMO) and the lowest unoccupied molecular orbital (LUMO) (Fukui, 1982).
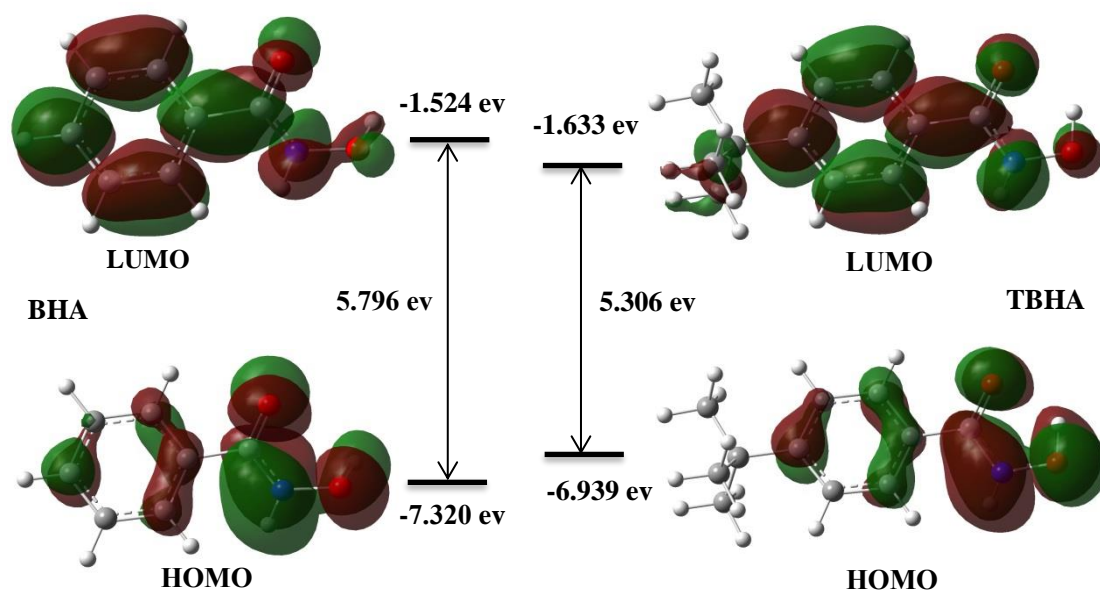

Fig. 5. Pictorial representations of the HOMO and the LUMO for BHA and TBHA

The energy gap between HOMO and LUMO serves as a stability index (Arjunan et al., 2014; El-Gammal et al., 2014). The large HOMO-LUMO energy gap of BHA (5.796 eV) and TBHA (5.306 eV) implies that they are kinetically stable molecules (Fig. 5). The highest occupied molecular orbital (electron donor) is mainly delocalized over the CO-NH-OH moiety for both BHA and TBHA, as shown in Fig. 5. The LUMO represents a π^* orbital, as evident from the presence of nodes in the benzene ring, as well as in the C-O and C-N bonds. The higher HOMO energy enables TBHA (-6.939 eV) stronger electron donating ability compared with BHA (-7.320 eV), i.e. stronger affinity to the mineral.

3.5 Binding model

Generally, the (O, O) chelation configuration is considered to be the most stable complex form when hydroxamic acids chelating metal ions (Kakkar et al., 2006). According to the above analysis, we also believe that the two oxygen atoms are the active center which donates electrons to the metal atoms on mineral surfaces during the flotation process. The diagrammatic sketch of the possible adsorption on rhodochrosite surface is shown in Fig. 6.
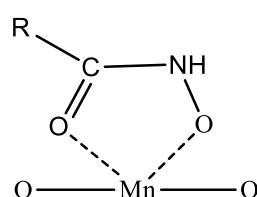

Fig. 6. Possible adsorption form of hydroxamic acid molecule on rhodochrosite surface, and R represents the alkyl group

The affinity of a collector to the metal ion can reflect its collecting ability to the corresponding mineral to a certain degree (Bag et al., 2011). The binding model between collectors and Mn^{2+} is simulated to discuss the collecting ability of collectors to rhodochrosite. The optimized geometries of the binding model are shown in Fig. 7, where the dashed lines represent the coordination bonds between oxygen atoms and Mn^{2+}. The complex in the binding model can be regarded as the simplified square configuration (only half square) that such configuration is the most stable configuration for the complex formed by the metal ion with d^5 electron configuration in low spin state based on the crystal field theory.
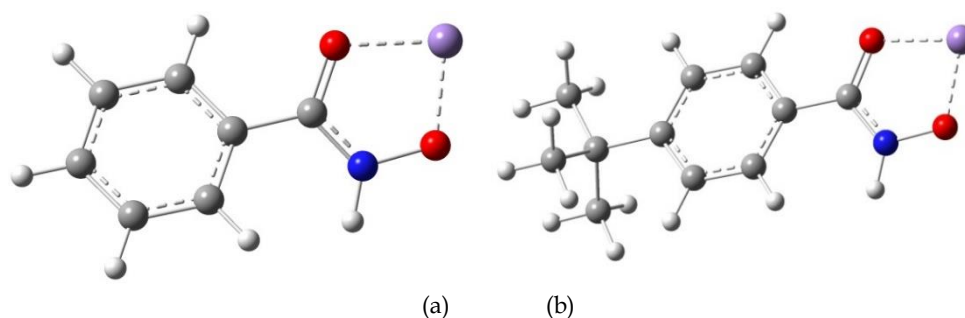

(a)   (b)

Fig. 7. Optimized geometries of the complexes of BHA-Mn (a) and TBHA-Mn (b)

To analyze the binding ability between the collectors and Mn^{2+}, bond order is used to compare the concerned bond strength in the collectors and the complexes. Bond order is the number of chemical bonds between a pair of atoms, which gives an indication of the stability and strength of a bond. There are many different quantum-chemical definitions of bond order among which the Wiberg bond index is very useful and extensively used in bond order analysis and is provided by the Gaussian package (Wiberg, 1968). The calculated results from natural bond orbital (NBO) analysis are listed in Table 3, the atom numbers are in accordance with that labeled in Fig. 2. The Wiberg bond indices of O-Mn in the complexes are 0.119 (0.287) for BHA and 0.198 (0.323) for TBHA, respectively, confirming that new

bonds form between oxygen atoms and manganese ions. The O-Mn bonds are regarded as coordination bonds owing to their smaller bond orders than that in hydroxamic groups. Furthermore, the bond strength of O-Mn in TBHA-Mn complex is stronger than the corresponding bond in BHA-Mn complex. Meanwhile the Wiberg bond indices of N2-O1 and C3-O4 become smaller and that of N2-C3 becomes bigger slightly, indicating that the electrons are better distributed in the functional group after oxygen atoms interacting with Mn^{2+}. The electron delocalization is favorable for the stability of collector-Mn complexes.

Table 3. Wiberg bond indices of the selected bonds in BHA, TBHA and the complexes (Å)

	O1-N2	N2-C3	C3-O4	O1-Mn	O4-Mn
BHA	1.008	1.225	1.590	-	-
BHA+Mn^{2+}	0.991	1.256	1.406	0.119	0.287
TBHA	1.010	1.205	1.564	-	-
TBHA+Mn^{2+}	0.973	1.229	1.399	0.198	0.323

Energies involved in the chelation reaction were calculated, including System energy (energy of the binding model, E_S), collector energy (E_C) and binding energy (E_B), as shown in Table 4. The binding energy of the collector and Mn^{2+} is calculated according to the equation: $E_B = E_S - (E_{Mn} + E_C)$, where E_{Mn} = -1150.560861 a.u.

Table 4. Calculated energies in the binding models

Energies	BHA	TBHA
E_C/(a.u.)	-475.798711	-633.082483
E_S/(a.u.)	-1626.476194	-1783.773271
E_B/(kJ/mol)	-306.191061	-341.123338

The binding energy of BHA or TBHA with Mn^{2+} is negative indicating that the reaction between them is feasible. The absolute values of the binding energy follow the sequence: TBHA > BHA, revealing that the combination between TBHA and Mn^{2+} is stronger, i.e. the conclusion could be drawn that the collecting ability of TBHA to rhodochrosite is stronger than that of BHA.

3.6 Micro flotation

Compared with BHA, the micro flotation of rhodochrosite using TBHA as the collector was carried out by investigating the effects of pH and collector dosage on the mineral recovery. The results are shown in Fig. 8 and Fig. 9, respectively.
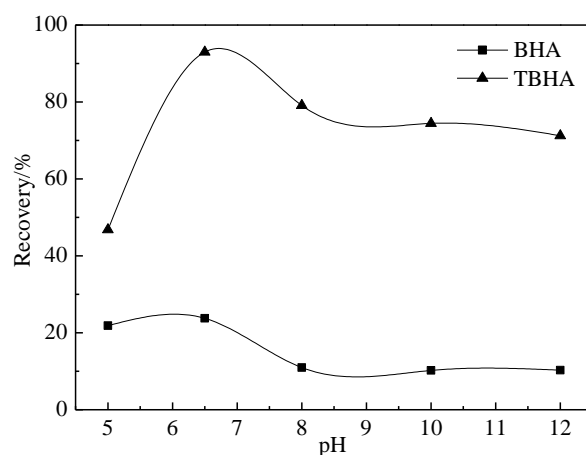

Fig. 8. Effect of pH on the recovery of rhodochrosite.
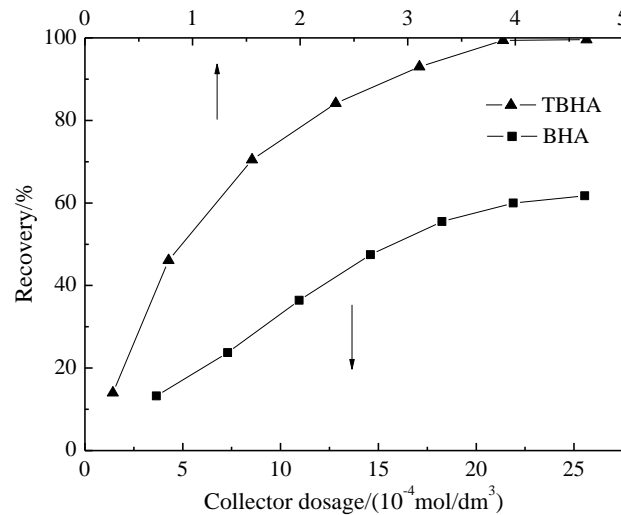BHA dosage =7.3×10⁻⁴ mol/dm³, TBHA dosage = 3.11×10⁻⁴ mol/dm³

Fig. 9. Effect of collector dosage on the recovery of rhodochrosite: pH=6.5

Considering the solubility of $MnCO_3$ in the acid environment, only the flotation responses at pH > 5 were studied, as shown in Fig. 8. The mineral recovery by TBHA is much stronger than that by BHA around pH = 5 ~ 12. For both BHA and TBHA the highest mineral recovery appears at about pH = 6.5, especially for the latter, the corresponding recovery can reach above 90%. Fig. 9 shows the flotation recovery of rhodochrosite at different collector dosages from $3.65 \times 10^{-4} \sim 2.55 \times 10^{-3}$ mol/dm³ for BHA and $0.26 \sim 4.66 \times 10^{-4}$ mol/dm³ for TBHA. The mineral recovery increases obviously with the increase of TBHA dosage and almost 99% mineral can be recovered when the dosage is above 3.89×10^{-4} mol/dm³. Meanwhile, the mineral recovery increases slowly with the increase of BHA dosage that the recovery is only about 60% when the dosage is 2.55×10^{-3} mol/dm³. The micro flotation data indicate that TBHA exhibits very strong collecting ability to rhodochrosite.

3.7 Electrokinetic property

Zeta potential reflects the electrokinetic change on mineral surfaces in aqueous solution. The zeta potentials of rhodochrosite in distilled water and in TBHA solution are displayed in Fig. 10. For rhodochrosite in water, the point of zero charge is located at pH = 6.52, i.e. the zeta potential is positive at pH < 6.5 and it is negative at pH > 6.5. This may be due to H^+ / OH^- ions adsorbed on mineral surfaces through O / Mn atoms of $MnCO_3$ at acid / alkaline environment, respectively. With the presence of TBHA, negative shifts can be observed in the zeta potential curve, that is, the anionic collectors can be adsorbed on mineral surfaces even that there are already H^+ or OH^- ions, indicating that the collector is probably chemically adsorbed on rhodochrosite surfaces.
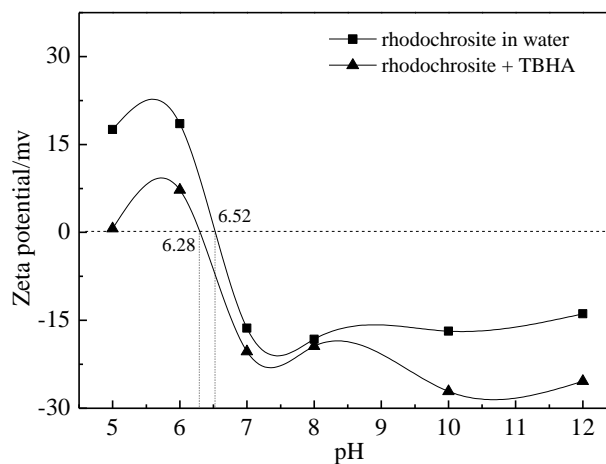

Fig. 10. Zeta potential of rhodochrosite in water and TBHA solution

3.8 XPS analysis

X-ray photoelectron spectroscopy was used to identify the elemental composition and analyze the surface chemistry of rhodochrosite in its as-received state, and after treatment by the collector. Fig. 11 shows the typical survey scan spectra over a binding energy range of 0 ~ 1300 eV.
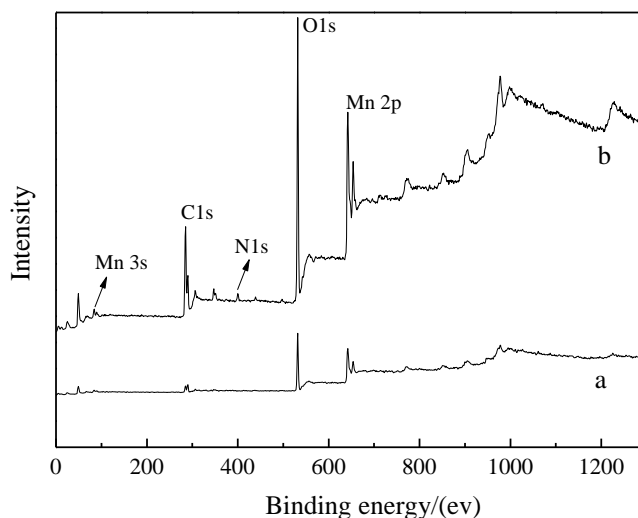

Fig. 11. The survey scan XPS of rhodochrosite before (a) and after (b) treatment

The XPS spectra in Fig. 11 show the expected elements from rhodochrosite, including Mn, C and O. In Fig. 11 (b), the signal of N 1s (400.75 eV) attributed to TBHA was detected for the treated rhodochrosite, confirming that TBHA is adsorbed on rhodochrosite surfaces.

The atomic concentrations of elements including Mn, C, O and N determined by microscopic analysis are summarized in Table 5, along with the atomic concentration ratio of these elements to Mn. The atomic concentration of N is 2.28% on the treated rhodochrosite surface. Meanwhile, the carbon concentration is increased, and the concentrations of manganese and oxygen are decreased. Considering the chemical formula of TBHA to be $C_{11}H_{15}NO_2$, the atomic concentration of C is much larger than O, so it would be anticipated that the atomic concentration of Mn and O are decreased due to the occupation of carbon on mineral surfaces. Actually, the adsorption of TBHA increases the atomic concentration ratio of C (O) to Mn from 1.98 (3.33) to 4.50 (4.01), and the extra C or O elements must be derived from the collector, making the chemical adsorption between TBHA and rhodochrosite more evident.

Table 5. Atomic compositions of elements on rhodochrosite surfaces

Rhodochrosite	Atomic concentration / %				Atomic concentration ratio to Mn			
	Mn 2p	C 1s	O 1s	N 1s	Mn 2p	C 1s	O 1s	N 1s
Before treatment	15.83	31.42	52.75	-	1.00	1.98	3.33	-
After treatment	10.28	46.24	41.20	2.28	1.00	4.50	4.01	0.22
Δ	-5.55	14.82	-11.55	2.28	0.00	2.52	0.68	0.22

Δ is defined as the value of before treatment minus that of after treatment by TBHA.

The valence states of surface species were further characterized by high-resolution XPS spectra for rhodochrosite before and after treatment by TBHA, as shown in Fig. 12.

In the XPS spectra for rhodochrosite, the peak for Mn 3s is located at 83.5 eV. After treated by TBHA, the binding energy of Mn 3s is decreased by 0.2 eV. The change of the binding energy of Mn 3s confirms that the chemical adsorption occurs between TBHA and rhodochrosite probably through Mn 3s accepting electrons donated from the collector.
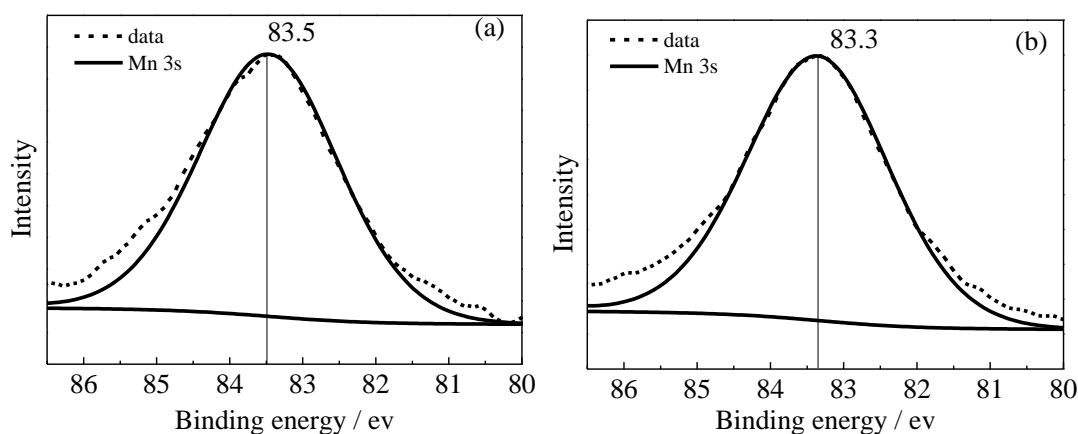
Fig. 12 Comparison of Mn 3s XPS spectra for rhodochrosite (a) and treated rhodochrosite (b)

4. Conclusions

Density functional calculations have been performed to study the structure and electronic property of the novel collector (TBHA) in the flotation of rhodochrosite. Experimental methods including micro flotation test, zeta potential measurement and X-ray photoelectron spectroscopy were carried out to discuss the collecting ability of TBHA to rhodochrosite and the adsorption mechanism. Compared with BHA, TBHA has larger HOMO energy and higher electron density on the oxygen atoms in the functional group, i.e. TBHA has stronger electron donating ability. The bond orders of the new formed bonds in TBHA-Mn^{2+} complex are bigger than the corresponding ones in BHA-Mn^{2+} complex, indicating a firmer combination of TBHA and Mn^{2+}. Meanwhile, the binding energy of TBHA and Mn^{2+} is larger than that of BHA and Mn^{2+}. TBHA exhibits excellent performance on the flotation of rhodochrosite that the mineral recovery is up to 99% when the dosage is 3.89 ×10^{-4} mol/dm^3 at pH=6.5. The electrokinetic property of rhodochrosite surfaces is changed by the adsorption of collector molecules as negative shifts occur for the zeta potential with the presence of TBHA. The chemical adsorption is confirmed between the collector and rhodochrosite from the XPS analyses. The atomic concentration ratios of C and O to Mn on the treated mineral surfaces were increased. Besides, the binding energy of Mn3s orbital was decreased by 0.2eV.

In summary, TBHA was proved to have stronger collecting ability to rhodochrosite than BHA by both theoretical and experimental investigations, i.e. the substitution of tert-butyl group on benzene ring significantly enhances the affinity of the hydroxamic acid to rhodochrosite. Consequently, TBHA is believed to be a justified candidate collector in the flotation of rhodochrosite or other oxidized ores.

References

ALI, O.Y., FRIDGEN, T.D., 2011. *Structures of electrosprayed Pb(Uracil-H)⁺ complexes by infrared multiple photon dissociation spectroscopy*. Int. J. Mass. Spectrom., 2-3, 167-174.

ARJUNAN, V., DEVI, L., SUBBALAKSHMI, R., RANI, T., MOHAN, S., 2014. *Synthesis, vibrational, NMR, quantum chemical and structure-activity relation studies of 2-hydroxy-4-methoxyacetophenone*. Spectrochim. Acta A, 130, 164-177.

ARORA, R., ISSAR, U., KAKKAR, R., 2017. *Theoretical study of the molecular structure and intramolecular proton transfer in benzohydroxamic acid*. Comput. Theor. Chem., 1105, 18-26.

AYERS, P.W., PARR, R.G., 2000. *Variational principles for describing chemical reactions: the Fukui function and chemical hardness revisited*. J. Am. Chem. Soc., 122, 2010-2018.

BAG, B., DAS, B., MISHRA, B.K., 2011. *Geometrical optimization of xanthate collectors with copper ions and their response to flotation*. Miner. Eng., 24, 760-765.

EL-GAMMAL, O.A., RAKHA, T.H., METWALLY, H.M., ABU El-REASH, G.M., 2014. *Synthesis, characterization, DFT and biological studies of isatinpicolinohydrazone and its Zn(II), Cd(II) and Hg(II) complexes*. Spectrochim. Acta A, 127, 144-156.

FARKAS, E., BETKA, D. CSAPO, E., BUGLYO, P., HAASE, W., SANNA, D., 2007. *Synthesis and characterization of Cu^{2+}, Ni^{2+} and Zn^{2+} binding capability of some amino- and imidazole hydroxamic acids: Effects of substitution of side chain amino-N for imidazole-N or hydroxamic-N-CH_3 on metal complexation*. Polyhedron, 26, 543-554.

FRISCH, M.J., TRUCKS, G.W., SCHLEGEL, H.B., SCUSERIA, G.E., ROBB, M.A., CHEESEMAN, J.R., SCALMANI, G., BARONE, V., MENNUCCI, B., PETERSSON, G.A., NAKATSUJI, H., CARICATO, M., LI, X., HRATCHIAN, H.P., IZMAYLOV, A.F., BLOINO, J., ZHENG, G., SONNENBERG, J.L., HADA, M., EHARA, M., TOYOTA, K., FUKUDA, R., HASEGAWA, J., ISHIDA, M., NAKAJIMA, T., HONDA, Y., KITAO, O., NAKAI, H., VREVEN, T., MONTGOMERY JR, J.A. , PERALTA, J.E., OGLIARO, F., BEARPARK, M., HEYD, J.J., BROTHERS, E., KUDIN, K.N., STAROVEROV, V.N., KOBAYASHI, R., NORMAND, J., RAGHAVACHARI, K., RENDELL, A., BURANT, J.C., IYENGAR, S.S., TOMASI, J., COSSI, M., REGA, N., MILLAM, J.M., KLENE, M., KNOX, J.E., CROSS, J.B., BAKKEN, V., ADAMO, C., JARAMILLO, J., GOMPERTS, R., STRATMANN, R.E., YAZYEV, O., AUSTIN, A.J., CAMMI, R., POMELLI, C., OCHTERSKI, J.W., MARTIN, R.L, MOROKUMA, K., ZAKRZEWSKI, V.G., VOTH, G.A., SALVADOR, P., DANNENBERG, J.J., DAPPRICH, S., DANIELS, A.D., FARKAS, O., FORESMAN, J.B., ORTIZ, J.V., CIOSLOWSKI, J., FOX, D.J., 2009. Gaussian Inc, Wallingford CT.

FUERSTENAU, D.W., SHIBATA, J., 1999. *On using electrokinetics to interpret the flotation and interfacial behavior of manganese dioxide*. Int. J. Miner. Process., 57(3), 205-217.

FUKUI, K., 1982. *Role of Frontier Orbitals in Chemical Reactions*. Science, 4574, 747-754.

GECE, G., BILGIC, S., 2010. *A theoretical study of some hydroxamic acids as corrosion inhibitors for carbon steel*. Corros. Sci., 10, 3304-3308.

GAO, Y.S., GAO, Z.Y., SUN, W., HU, Y.H., 2016a. *Selective flotation of scheelite from calcite: A novel reagent scheme*. International Journal of Mineral Processing, 154, 10-15.

GAO, Z.Y., GAO, Y.S., ZHU, Y.Y., HU, Y.H., SUN, W., 2016b. *Selective flotation of calcite from fluorite: a novel reagent schedule*. Minerals, 6(4), 114.

GRIFFITH, D.M., SZOCS, B., KEOGH, T. SUPONITSKY, K.Y., FARKAS, E., BUGLYO, P., MARMION, C.J., 2011. *Suberoylanilide hydroxamic acid, a potent histone deacetylase inhibitor; its X-ray crystal structure and solid state and solution studies of its Zn(II), Ni(II), Cu(II) and Fe(III) complexes*. J. Inorg. Biochem, 6, 763-769.

HAN, H.S., HU, Y.H., SUN, W., LI, X.D., CAO, C.G., LIU, R.Q., YUE, T., MENG, X.S., GUO, Y.Z., WANG, J.J., GAO, Z.Y., CHEN, P., HUANG, W.S., LIU, J., XIE, J.W., CHEN, Y.L., 2017. *Fatty acid flotation versus BHA flotation of tungsten minerals and their performance in flotation practice*. Int. J. Miner. Process., 159, 22-29.

JORDENS, A., MARION, C., GRAMMATIKOPOULOS, T., HART, B., WATERS, K.E., 2016. *Beneficiation of the Nechalacho rare earth deposit: Flotation response using benzohydroxamic acid*. Miner. Eng., 99, 158-169.

KAKKAR, R., GROVER, R., GAHLOT, P., 2006. *Density functional study of the properties of isomeric aminophenylhydroxamic acids and their copper (II) complexes*. Polyhedron, 3, 759-766.

LIU, G.Y., ZENG, H.B., LU, Q.Y., ZHONG, H., CHOI, P., XU, Z.H., 2012. *Adsorption of mercaptobenzoheterocyclic compounds on sulfide mineral surfaces: A density functional theory study of structure–reactivity relations*. Colloid. Surface. A, 409, 1-9.

LIU, G.Y., ZHONG, H., DAI, T.G., 2006. *The separation of Cu/Fe sulfide minerals at slightly alkaline conditions by using ethoxycarbonyl thionocarbamates as collectors: Theory and practice*. Miner. Eng., 13, 1380-1384.

NAGARAJ, D.R., FARINATO, R.S., 2016. *Evolution of flotation chemistry and chemicals: A century of innovations and the lingering challenges*. Miner. Eng., 96-97, 2-14.

PARR, R.G., YANG, W., 1984. *Density functional approach to the frontier-electron theory of chemical reactivity*. J. Am. Chem. Soc., 106, 4049-4050.

SOUSA, R., FUTURO, A., PIRES, C.S., LEITE, M.M., 2017. *Froth flotation of Aljustrel sulphide complex ore*. Physicochem. Probl. Miner. Process., 2, 758-769.

WIBERG, K.B., 1968. *Application of the Pople-Santry-Segal CNDO Method to the cyclopropylcarbinyl and cyclobutyl cation and to bicyclobutane*. Tetrahedron, 24, 1083-1096.

Wu X.Q., Zhu J.G., 2006. *Selective flotation of cassiterite with benzohydroxamic acid*. Miner. Eng., 19, 1410-1417.

YANG, H., FAIRBRIDGE, C., Ring, Z., 2003. *Adsorption of dibenzothiophene derivatives over a MoS$_2$ nanoclusters a density functional theory study of structure-reactivity relations*. Energ. Fuel., 17, 387-398.

ZHAO, G., ZHONG, H., QIU X.Y., WANG, S., GAO, Y.D., DAI, Z.L., HUANG, J.P., LIU, G.Y., 2013. *The DFT study of cyclohexyl hydroxamic acid as a collector in scheelite flotation*. Miner. Eng., 49, 54-60.

ZHOU, F., CHEN, T., YAN, C.J., LIANG, H., CHEN, T., LI, D., WANG, Q.Y., 2015b. *The flotation of low-grade manganese ore using a novel linoleate hydroxamic acid*. Colloid. Surface. A, 466, 1-9.

ZHOU, F., YAN, C.J., WABG, H.Q., SUN, Q., WANG, Q.Y., ALSHAMERI, A., 2015a. *Flotation behavior of four C18 hydroxamic acids as collectors of rhodochrosite*. Miner. Eng., 78, 15-20.